

Review

# Tautomerism of $\beta$ -Diketones and $\beta$ -Thioxoketones

Poul Erik Hansen 

Department of Science and Environment, Roskilde University, DK-4000 Roskilde, Denmark; poulerik@ruc.dk

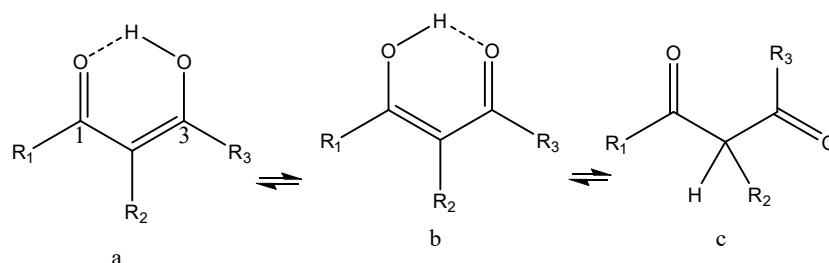
**Abstract:** The present overview concentrates on recent developments of tautomerism of  $\beta$ -diketones and  $\beta$ -thioxoketones, both in solution and in the solid state. In particular, the latter has been a matter of debate and unresolved problems. Measurements of  $^{13}\text{C}$ ,  $^{17}\text{O}$ , and  $^2\text{H}$  chemical shifts have been used. Deuterium isotope effects on chemical shifts are proposed as a tool in the study of this problem. Photoconversion of  $\beta$ -diketones and  $\beta$ -thioxoketones are discussed in detail, and the incorporation of  $\beta$ -diketones into molecules with fluorescent properties is assessed. Finally, docking studies of  $\beta$ -diketones are scrutinized with an emphasis on correct tautomeric structures and knowledge about barriers to interconversion of tautomers.

**Keywords:** tautomerism; hydrogen bonding; biological effects; isotope effects on chemical shifts; photochemistry

## 1. Introduction

### 1.1. $\beta$ -Diketones

$\beta$ -diketones is a very broad subject. The present paper concentrates on some recent developments, primarily since 2008. The  $\beta$ -diketones (see Scheme 1) are a very versatile group of molecules that easily can be synthesized [1], and hence be tailored to fulfill different purposes. In addition, they can be isolated as natural products often with extraordinary structures [2].  $\beta$ -Diketones are very good synthons [1,3]; e.g., they can be converted into  $\beta$ -thioxoketones (Scheme 2). In addition, they are known to have useful biological effects [2]. A well known example is curcumin and derivatives thereof (Figure 1) [4–6]. The physical properties are related to uptake [7].  $\beta$ -Diketones can form a large number of metal complexes [8]. A group of compounds with similar properties is the  $\beta$ -trioxoketones [9], and a well-studied case is usnic acid [9]. Linear  $\beta$ -diketones may exist as different tautomers (enol and keto- forms, Scheme 1). The key features of the enol forms are strong intramolecular hydrogen bonds, tautomeric forms (see Scheme 1), and a very low barrier to interconversion between the enolic forms.



**Scheme 1.** Tautomers of  $\beta$ -diketones. **a** and **b** are enol forms, **c** is the diketo-form.



**Citation:** Hansen, P.E. Tautomerism of  $\beta$ -Diketones and  $\beta$ -Thioxoketones. *Encyclopedia* **2023**, *3*, 182–201. <https://doi.org/10.3390/encyclopedia3010013>

Academic Editors:  
Francesco Cacciola, Petr Česla,  
Drago Beslo and Raffaele Barretta

Received: 20 November 2022

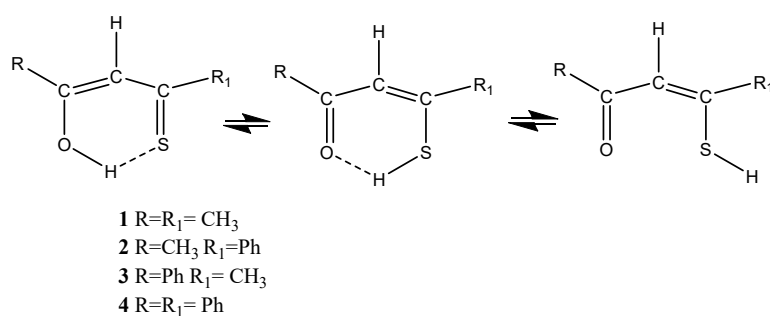
Revised: 26 January 2023

Accepted: 28 January 2023

Published: 30 January 2023



**Copyright:** © 2023 by the author. Licensee MDPI, Basel, Switzerland. This article is an open access article distributed under the terms and conditions of the Creative Commons Attribution (CC BY) license (<https://creativecommons.org/licenses/by/4.0/>).



**Scheme 2.** Tautomers of  $\beta$ -thioxoketones plus the open form.

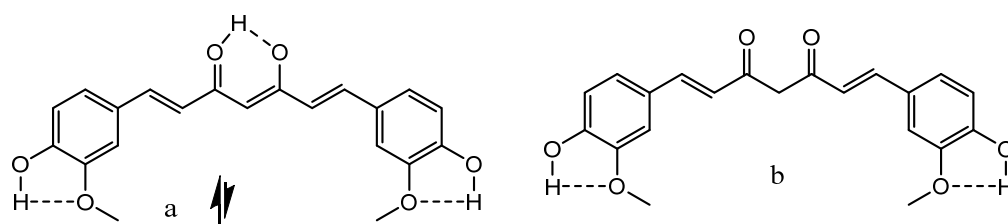


**Figure 1.** Curcumin. The second enolic tautomer is similar to acetylacetone (see Scheme 1). (a) is the enol form, (b) the diketo-form.

### 1.2. $\beta$ -Thioxoketones

$\beta$ -Thioxoketones (see Scheme 2) and  $\beta$ -diketones are in many ways complementary. Both types display strong intramolecular hydrogen bonds, show tautomerism, and have low barriers to interconversion [10]. The  $\beta$ -thioxoketones are by nature asymmetric and may actually show an open form (Scheme 2).  $\beta$ -Thioxoketones are colored, and they provide a way of exciting the molecules with visible light sources.  $\beta$ -thioxoketones form, by their nature, very good metal complexes [11], some of which also show biological effects [12].  $\beta$ -thioxoketones can be synthesized from  $\beta$ -diketones [13] and also from salicylaldehyde [14].

The present review will concentrate on structural studies, including tautomers in the liquid and solid state. The importance of low barrier hydrogen bonds (LBHB) will be discussed and hydrogen bond strength, docking studies, and photoconversion will be assessed. The primary experimental methods treated are NMR and isotope effects on chemical shifts, X-ray structures, and infra-red spectroscopy. The experimental techniques are supplemented by theoretical calculations, including Density Functional Theory (DFT) calculations [15,16]. In particular, the low barriers call for advanced calculations both in the liquid and in the solid state.

## 2. Tautomerism

### 2.1. Gas Phase

Acac was studied in the gas phase using electron diffraction (GED). At 300 K, it was found to be fully in the keto-enol form. The percentage was reduced to 64% of the enol at 671 K. The keto-enol tautomer possesses C<sub>s</sub> symmetry with a planar ring and strongly asymmetric hydrogen bond. The experimental parameters could be reproduced well by B3LYP/aug-cc-pVTZ and MP2/cc-pVTZ calculations [17]. Dibenzoylmethane showed 100% keto-enol tautomer at 380K. [18] 3-chloro-2,4-pentanedione showed 100% at 269 K [19], as did 5-hydroxy-2,2,6,6-tetramethyl-3-heptanone [20].

### 2.2. Liquid State

Linear  $\beta$ -diketones show two types of tautomers, as shown in Scheme 1. The OH to CH tautomerism is slow as both are observed in <sup>1</sup>H NMR spectra. The barrier to interconversion is high [10] (for a discussion of barriers to interconversion see below and Docking), whereas the OH to OH tautomerism is very fast as the barrier to interconversion is so low that the

system can be classified as “low barrier hydrogen bond” (LBHB are defined as system with matching pKa for the donor and acceptor) [21].  $\beta$ -Diketones may serve as a testing ground for this kind of hydrogen bond. The ratio between the enol and keto-forms depends on the polarity of the solvent [22] and on the character of the substituents  $R_1$ ,  $R_2$ , and  $R_3$ ; thus, a number of properties can be tuned by a change of substituents [23–25]. The enol content increases as the size of  $R_1$  and  $R_3$  increases, whereas the diketo-form increases with the size of  $R_2$ . Sloop et al. investigated electron deficient aryl  $\beta$ -diketones and found that in the liquid state, that the compound (Scheme 1,  $R_1 = \text{Ph}$ ,  $R_2 = \text{H}$ , and  $R_3 = \text{CF}_3$ ) existed primarily in the enol form with the OH hydrogen bonding to the C=O next to  $\text{CF}_3$ , whereas the corresponding compound (Scheme 1,  $R_1 = \text{Ph}$ ,  $R_2 = \text{F}$ , and  $R_3 = \text{CF}_3$ ) with fluorine at the central carbon existed primarily at the diketo-form [26]. Belova et al. concluded that substituents such as H,  $\text{CH}_3$ ,  $\text{CF}_3$ , and  $\text{C}(\text{CH}_3)_3$  strongly favor the enol tautomer, whereas substituents such as F, Cl,  $\text{OCH}_3$ , and  $\text{NH}_2$  favor the keto-form. [27] The keto-form is favored by methoxy groups in the para-position [28]. The effect of water has also been investigated [29]. Computational results showed further that the polar solvent dioxane enhances the enol form of these 12 molecules more effectively than water and chloroform media [30]. Acetylacetone, trifluoroacetylacetone, and hexafluoroacetylacetone were studied in supercritical  $\text{CO}_2$  solutions at pressures up to 3.1 kbar. The keto-form was found to be favored at high pressure and low temperature [31]. Keto-enol equilibria were also studied based on electron delocalization indices and delocalization tensor density [32].

The enol and keto-forms have different structures (see Scheme 1) and have different dipole moments [33]. Keto-enol equilibria may also be modified by inclusion into nanospaces [34] or calix [4] arenes [29].

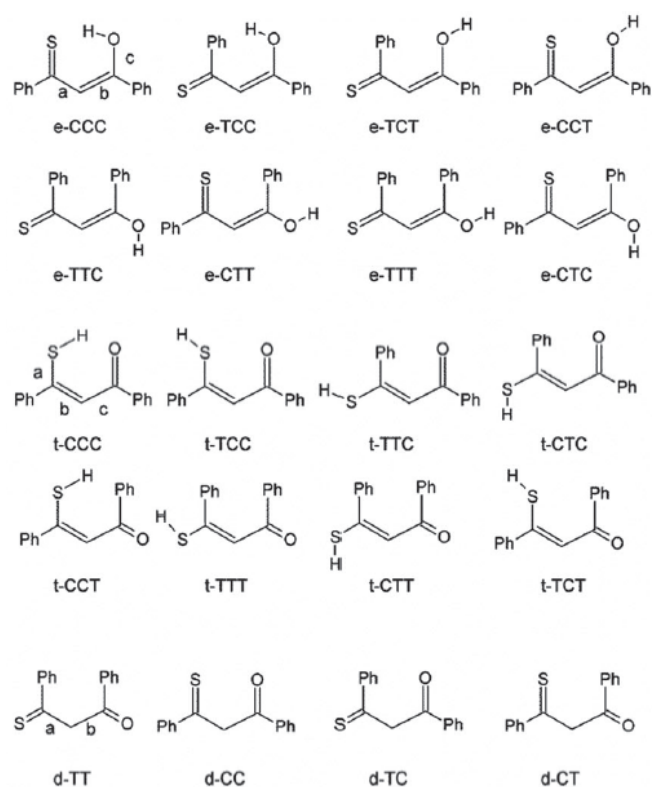
Tautomeric analyses of a series of substituted  $\beta$ -diketones ((3-methylthio)-2,4-pentanedione [35], (3-phenylthio)-2,4-pentanedione [36], 3-bromo-2,4-pentanedione [37], and 1,1,1-trifluoro-2,4-pentanedione [38] have been performed in order to obtain hydrogen bond strengths. A large number of curcumin analogues have been studied by  $^{13}\text{C}$  NMR and DFT calculations in order to determine equilibrium constants of the keto-enol equilibrium [39]. Curcumin analogues have recently been investigated by applying quantitative structure–activity relationship and absorption, distribution, metabolism, and excretion (ADME) approaches. The enol-form is generally the more effective against cancer, especially prostate cancer. The more OH and  $\text{OCH}_3$  groups, the better [40].

Mehrani et al. have investigated a large number of functional and basis sets to obtain the energy of tautomers of acetylacetone also including methods such as the polarizable continuum model (PCM) [41], conductor-like polarizable continuum model (CPCM) [42], and solvent model density (SMD) [43] models to take into account solvent effects. Sixteen different acetylacetone (acac) solutions and gas phases were investigated [44]. The conclusion was that G3B3 and G3MP2B3 functionals gave reasonable results compared to experimental values and the best result was obtained using B2LYP/6-31+G(2d,p) and CBS-QB3.

Roy et al. [33] found that for acetylacetone, the DFT functional B3LYP with the basis set 6-311G(d) gave better thermodynamic results than MP2 with the same basis set. They also calculated the interconversion barrier as  $\sim 59 \text{ kcal mol}^{-1}$  in a vacuum. This number decreases somewhat in polar solvents. A topological and energy partition analysis of acac was done in the framework of the Quantum Theory of Atoms in Molecules (QTAIM) [45]. This showed that the activation barrier energy decreases from the gas phase to clusters with up to three water molecules surrounding the acac and increases when four water molecules were included [46].

An example of theoretical calculations not properly rooted in experimental facts is the report based on DFT calculations, claiming that 1,3,5-trihydroxy-2,4,6-trihydroxybenzene is tautomeric [47]. This was followingly shown not to be the case based on deuterium isotope effects on  $^{13}\text{C}$  chemical shifts [48].

$\beta$ -Thioxoketones show only “enol” forms (see Scheme 2). However, in this case, an open form is also possible (see Figure 2). A large number of tautomers, rotamers, and isomers are possible, as seen in Scheme 3.



**Scheme 3.** Tautomers, rotamers, and isomers of  $\beta$ -thioxoketones. Abbreviations: e = enol, d = diketo; XXX: The last X refers to the orientation of the OH or C=O bond; the middle X to the conformation around the double bond, the first X to the orientation of the SH bond. Taken from Ref. [49].

### 2.3. Solid State

Kong et al. [50] wrote “a unified picture of the H atom behavior in a LBHB hydrogen bonded system, that can reconcile diffraction and solid-state NMR data is still lacking”. This is clearly the case as will be obvious from the following.

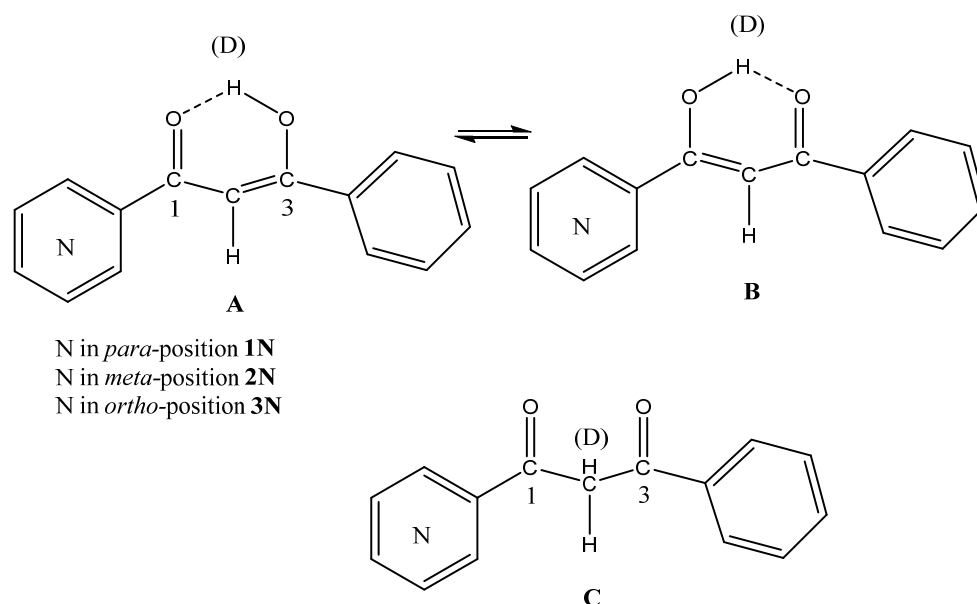
X-ray studies of  $\beta$ -diketones can be done at low temperature; however, this may change the position of the OH proton as nicely demonstrated in the study of benzoylacetone [51]. The crystal structure of dibenzoylmethane shows that the carbonyl carbons of the enol form are different due to twisting of one of the benzene rings. In addition to X-ray studies, a neutron diffraction study was also performed. The latter showed that the proton is located asymmetrical and the position is insensitive to temperature. The X-ray measurement showed “a migration of the bonding density from an asymmetric position at low temperature to an almost centered position at RT” [52]. Ultra-fast electron diffraction yielded an asymmetric ground-state structure [53]. As mentioned above, Kong et al. [49] investigated dibenzoylmethane as well as curcumin using both  $^{17}\text{O}$ ,  $^2\text{H}$ , and  $^{13}\text{C}$  solid-state NMR combined with CASTEP (Cambridge Sequential Total Energy Package) [54] combined with *ab initio* molecular dynamics (MD) simulations. Two possible solutions, either tautomerism or a single well potential, were arrived at.

Conradie et al. [55] showed that the enol proton is on the same side as the thienyl group in 1-phenyl-3-(2-thionyl)1,3-propanedione from an X-ray study at 100K. This enables for the determination of the conversion rate to the keto-form in solution. Nieto et al. [56] studied the X-ray structures of a series of curcumins at ambient temperature and found that only one of the enol forms were present. The same is true for 1-aryl-1,3-diketone malonates. Four compounds (Scheme 1,  $\text{R}_1 = \text{Ph}$ , 4- $\text{NO}_2$ , Ph, 4-MePh, and 2-naphthyl,  $\text{R}_2 = \text{H}$ , and  $\text{R}_3 = \text{CH}_2\text{CH}_2\text{CH}(\text{COOMe})_2$ ) were investigated. The nitro and the naphthalene derivative showed delocalization parameters of 0.23 and 0.28, which were somewhat less than the 0.32 expected for a true keto-enol form. Parameters for a series of  $\beta$ -diketones are compared in this paper [57].

Sloop et al. [26] did not find a difference between the liquid (see above) and the solid state for fluorinated  $\beta$ -diketones. 1,3-bis(1-adamantyl)propan-1,3-diones with phenyl substituents at C-2 showed only the diketo-form [58]. X-ray studies of hexafluoroacetone crystals grown in situ by means of the zone-melting technique at 93K, showed clear evidence for distinguishable O-1-H and H...O-2 bonds [59]. The structure of 1-(thiophen-2-yl)-3-(thiophen-3-yl)propane-1,3-dione showed a keto-enol form with the OH group close to the 3-thiophene ring [60].

1-phenyl-1,3-butadione and 1-deuteroxy-2-deutero-1-phenylbut-1-en-3-one crystals has been carried out at 160 K and 300 K on the Carr-Parrinello molecular dynamics (CPMD) [61] level and at 300 K on the path integral molecular dynamics (PIMD) method [62] level. The analysis of the two-dimensional free-energy landscape of reaction coordinates and RO...O distances shows that the hydrogen (deuterium) between the two oxygen atoms adopts a slightly asymmetrical position [63].

Deuterium isotope effects on  $^{13}\text{C}$  chemical shifts (see Experimental) have been used in a few cases to investigate tautomeric equilibria in the solid state. These studies can be done at ambient temperature. An example of the use of deuterium isotope effects on  $^{13}\text{C}$  chemical shifts is in pyridoylbenzoyl  $\beta$ -diketones (Scheme 4) [64]. For **2N** and **3N** (Scheme 4), C-1 is shifted 0.8 and 1.2 ppm to lower frequency upon deuteration, whereas C-3 shows no isotope effect. This points towards the B-form being dominant. For **1N**, the effect leads for C-1 to a change of 2.4 ppm to a higher frequency, whereas C-3 is shifted from 0.7 ppm to lower frequency. As the average is very different from 0.6 ppm (the average found in solution), it was suggested that crystal effects due to deuteration was at play. The findings for **2N** and **3N** in the solid is opposite to those observed in the liquid state [64]. The X-ray structures have been determined; for **1N** and **2N**, the proton is closest to the pyridine ring, but for **3N**, it is closest to the phenyl ring [65]. The pyridoylbenzoyl  $\beta$ -diketones were also co-crystallized with perfluorinated iodobenzenes to give the tautomer with the OH group next to the pyridine ring (see Figure 2) [66]. Studies of other  $\beta$ -diketones are under way [67].



**Scheme 4.** Tautomerism of pyridoylbenzoyl  $\beta$ -diketones. Only very small amounts of the diketo-form were found.

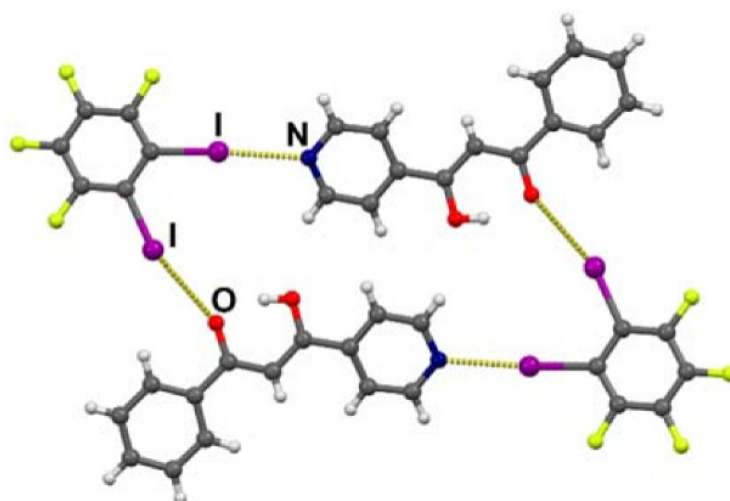


**Figure 2.** Co-crystal of 3N with 1,2-di-iodo-3,4,5,6-tetrafluorobenzene. Taken from Ref. [66].

As is evident from the text above, more tools are desirable in the study of tautomerism of  $\beta$ -diketones in the solid state. One such tool could be deuterium isotope effects on  $^{17}\text{O}$  chemical shifts. An example in the liquid state is in 1-(2-hydroxycyclohex-1-en-1-yl)ethan-1-one deuteriated at the OH proton. Two characteristics, including the large effects and opposite signs of  $^1\Delta^{17}\text{O}(\text{D}) = 9.63$  ppm and  $^5\Delta^{17}\text{O}(\text{D}) = -11.65$  ppm are useful [68]. The large effects make it likely to observe the effects in the solid state, at least for asymmetric  $\beta$ -diketones.

First of all, the X-ray structures of  $\beta$ -thioxoketones show no diketo-forms. Secondly, the enol-thione form is the only enolic form in the solid state [69]. This was confirmed for thiodibenzoylmethane (see Scheme 2) using deuterium isotope effects on  $^{13}\text{C}$  chemical shifts. For deuteriated  $\beta$ -thiodibenzoylmethane in the solid state, the C=S carbon showed an isotope effect of 1.2 ppm at  $-40$  °C, whereas the carbon with the OH group attached showed an effect of 0.8 ppm. Both effects were ascribed to intrinsic effects. In other words, no tautomeric equilibrium was formed. Measuring the  $^{13}\text{C}$  chemical shift is following a way to obtain reference  $^{13}\text{C}$  chemical shifts for the enol-thione form.

### 3. Photoconversion

#### 3.1. $\beta$ -Diketones

Dibenzoylmethanes (Scheme 1,  $R_1=R_3=\text{Ph-4R}$  and  $R_2=\text{H}$  and  $R_2=\text{F}$ ) can be converted fully into the diketo-form by irradiation at 365 nm at RT in acetonitrile. Subsequently, the diketo-form will return to the initial 90% keto-enol form in the dark. The back reaction can be promoted by additives; water is especially effective [70]. A theoretical study of the sunscreen, Avobenzone (4-tert-butyl-4-methoxydibenzoylmethane), showed that irradiation leads both to the diketo-form, an open form (similar to that seen for  $\beta$ -thioxoketones in Scheme 2), and cis-trans isomerisations [71]. Other compounds, such as difuruyl and ditheonyl methanes (Scheme 1,  $R_1 = R_3 = \text{furane}$  or thiophene and  $R_2 = \text{CH}_3$  or  $n\text{-C}_3\text{H}_7$ ), were converted into the diketone form upon irradiation. The diketo-form returned to the keto-enol form in the dark after some days [72]. Recently, triphenylamine (TPA) with  $\beta$ -diketone side chains (Figure 3) was studied by ultrafast spectroscopy. Transient spectra data showed that an intramolecular charge transfer (ICT) takes place from TPA units to  $\beta$ -diketones units after photoexcitation [73].

Ultrafast electron diffraction studies of acac showed that the chelate proton is clearly at one oxygen at the time in the electronic ground state, whereas it is at the center of the hydrogen bonded system in the excited state [53]. Vertical laser excitation of the p-p band ( $S_0$  to  $S_2$ ) leads to excited state intramolecular proton transfer (ESIPT). The process is more complex than simple ESIPT, as seen in Scheme 5.

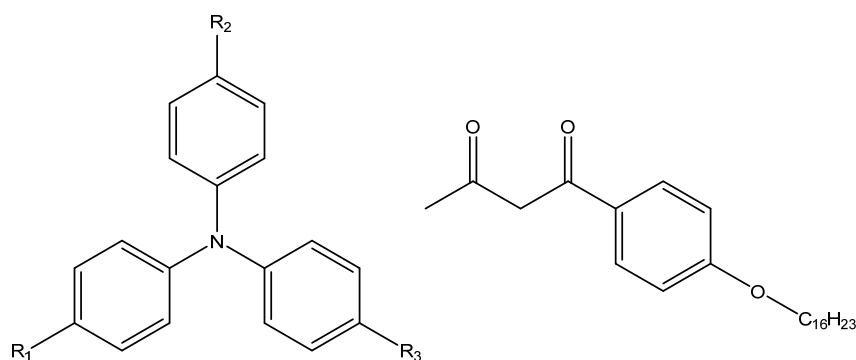
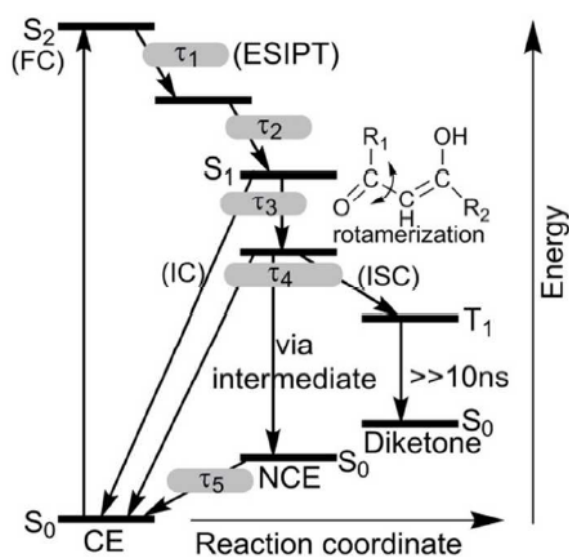


**Figure 3.**  $R_1$ ,  $R_2$ , and  $R_3$  can either be the substituent to the right or H.



**Scheme 5.** Excitation scheme for a  $\beta$ -diketone. From Ref. [74]. With permission from the Royal Society of Chemistry.

An excitation study of the enol form of 2-acetylindan-1,3-dione (AID) [75] leads to fluorescence, as seen in Figure 4. 2-acetylindan-1,3-dione is found to exist exclusively in the enol form. The first excitation at 300 nm is to  $S_1^A$ , which initiates ESIPT to tautomer B (Scheme 6).

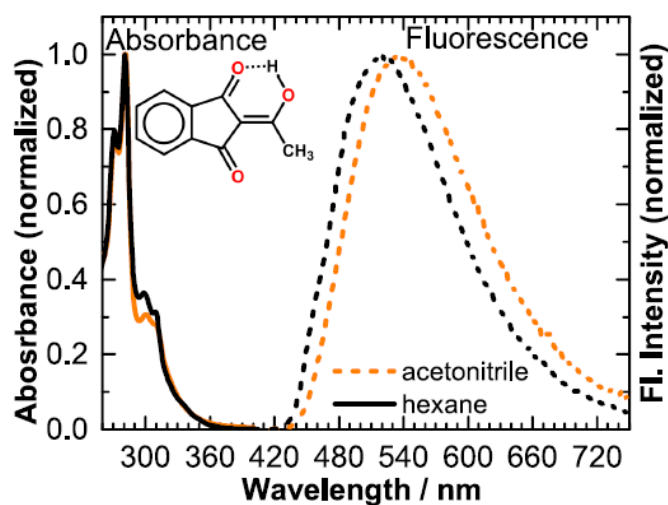
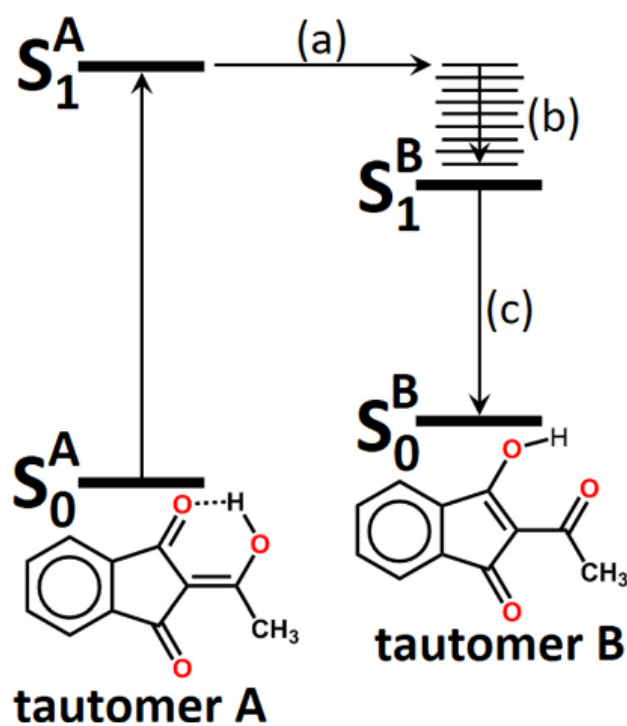


**Figure 4.** Absorption (solid) and emission spectra (dashed, excitation wavelength 300 nm). Taken from Ref. [75], licensed under a Creative Commons Attribution (CC BY) license.



**Scheme 6.** Energy diagram for excitation of 2-acetylindan-1,3-dione. Taken from Ref. [75], licensed under a Creative Commons Attribution (CC BY) license.

This is followed by vibrational relaxation; from the  $S_1^B$  state, it is relaxed to the ground state  $S_0^B$ . The ground state relaxes back to tautomer A. One drawback of this system is that a cis-trans isomerization is invisible. Furthermore, the ESIPT product cannot be isolated.

Li et al. [76] investigated the ESIPT using DFT, time-dependent DFT, and DFT in two solvents, hexane and acetonitrile, and explained the experimental results described by Verma et al.

ESIPT has been demonstrated in OLED's, as seen in Figure 5, using the PXZDO molecule of Figure 6 [77].

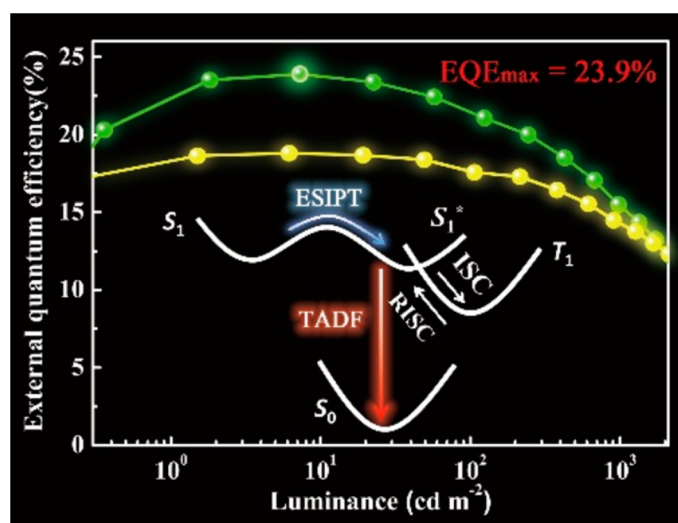


**Figure 5.** Efficiency scheme. TADF (thermally activated delayed fluorescence, ISC, intersystem crossing). Yellow data are for PXZDO. Taken from Ref. [77] with permission from the American Chemical Society.

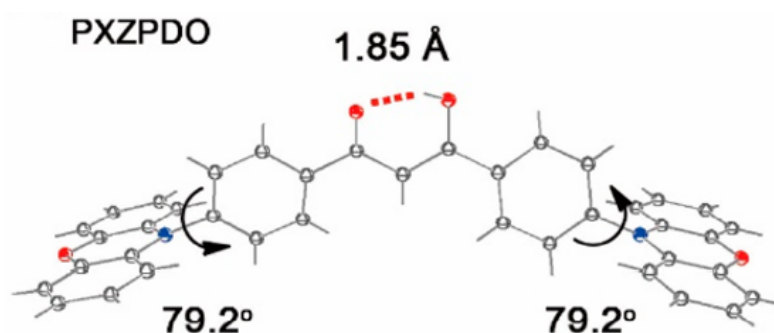


**Figure 6.** Enolic structure of 1,3-bis(4(10H-phenoazin-10-yl)phenyl)3-hydroxyprop-2-en-1-one (PXZDO). Taken from Ref. [77] with permission from the American Chemical Society.

The molecules are of the D-P-A-P-D type (D = donor, A = acceptor). As the core of molecules are  $\beta$ -diketones, they may exist both as enols and ketones.

A number of recent papers discuss fluorescence. An example is the modified boron-difluorid dipyrromethene (BODIPY), as seen in Figure 7. Solvent dependence was investigated and for hydrogen bonding solvents interactions were found in the excited state between the OH group and the solvent [78]. The structure of DPHND (Figure 8) is held planar by the extra hydrogen bond. The molecular planarity is important for the generation of highly emissive crystals [79,80]. The hydrogen bond motif is akin to that of tetracycline [9]. A slightly different construction, alkene-linked 1,1'-bi-2-naphthol- $\beta$ -diketones, was also shown to be highly emissive [81].

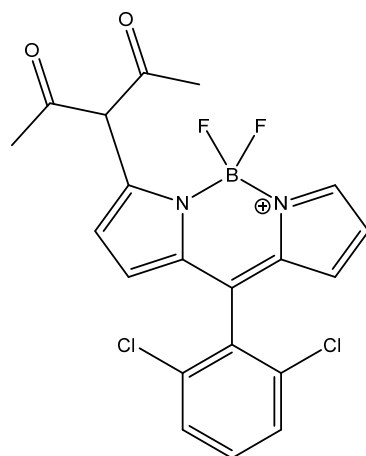


**Figure 7.** Modified BODIPY. The keto-form is shown; however, an equilibrium exists between the enol and keto-form.

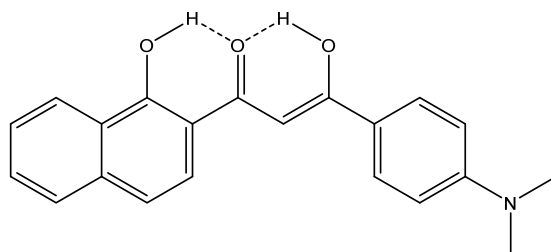


**Figure 8.** Structure of (Z)-3-(4-(dimethylamino)phenyl)-3-hydroxy-1-(1-hydroxynaphthalen-2-yl)prop-2-en-1-one (DPHND).

### 3.2. $\beta$ -Thioxoketones

The  $\beta$ -thioxoketones are characterized by a tautomeric equilibrium between an enol-thio ketone and a keto-thiol form (see Scheme 2). As has been discussed earlier, an open

form may also exist. The OH forms a very strong hydrogen bond (chemical shift  $\sim 17$  ppm), whereas the SH group only forms a weak hydrogen bond (chemical shift  $\sim 3\text{--}5$  ppm) [82]. However, due to the low barrier [49] between the two tautomers, only an averaged NMR spectrum is observed.

To study the photoconversion of  $\beta$ -thioxoketones, it is necessary to know the ground state structure, in this case the tautomeric situation, and as excitation experiments are often done at low temperature, the ground state situation at low temperatures must be known. Furthermore, the substituent  $R_1$  and  $R_2$  may also play a role, as well as the solvent. Oxygen should be avoided as this may lead to unwanted products and not only quenching.

Despite the fact that NMR leads to averaged parameters (see previously), NMR is a very suitable tool in the study of the tautomerism of  $\beta$ -thioxoketones. The reason is that the difference between the OH and the SH chemical shifts is very large (see above). The same is true for the C=O, COH, and the C=S, CSH pairs, when measuring  $^{13}\text{C}$  NMR spectra. A variable temperature study gave the following values for **1**.  $\Delta(\text{C}=\text{S}) = 217$  ppm,  $\delta(\text{CSH}) = 163$  ppm,  $\delta(\text{C}=\text{O}) = 198$  ppm, and  $\delta(\text{COH}) = 186$  ppm [82].

For the monothioacetylacetonone (**1**), an open form is indicated by the fact that a plot of XH(OH,SH) chemical shifts vs. temperature showed a broadening at 200 K. For **1** and **2**, a plot of deuterium isotope effects (XH partially deuteriated) vs. temperature (Figure 9) showed a large drop around, again indicating the presence of the open form.

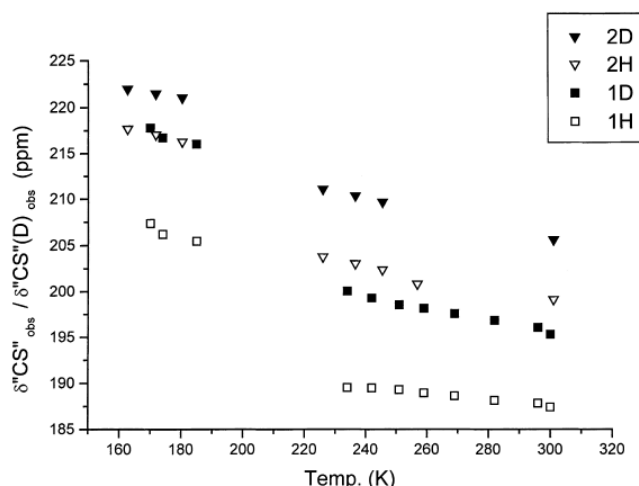


**Figure 9.** Plot of “CS” chemical shift vs. temperature. Taken from Ref. [82] with permission from Elsevier.

For **3** and **4**, this is not the case (not shown). The cyclic  $\beta$ -thioxoketone **5** (Figure 10) showed no discontinuity in the XH spectrum vs. temperature [83]. Thus, **4** and **5** are suitable for photochemical conversion studies; **5** has the advantage that the oxygen is part of the ring, eliminating the possibility that the oxygen can be “trans”, as seen for **4**.

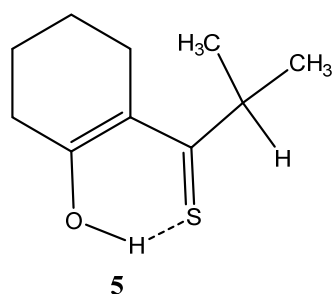


**Figure 10.** Structure of compound **5**.

The UV-vis spectrum of **4** is shown in Figure 11. The band at 410 nm is ascribed to the  $\pi,\pi^*$  transition. The figure shows which bands disappear upon irradiation at 410 nm [84].

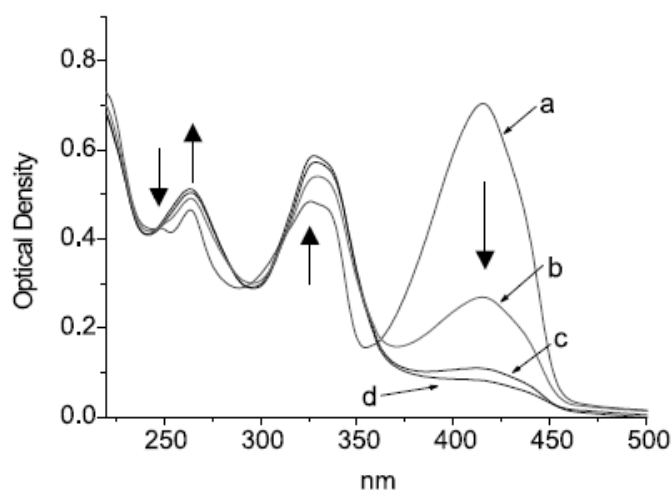


**Figure 11.** UV spectrum of **4**, trace a in 3-methylpentane at 90 K. b, c, d is after irradiation at 410 nm for 10, 20, and 30 min. Taken from Ref. [84] with permission from Elsevier.

The UV spectrum show disappearance of the C=S chromophore on irradiation at 410 nm. This corresponds to the formation of the open form (t-TCC, Scheme 1). This was also demonstrated upon irradiation of **4** in an argon matrix [84]. This was very clearly seen by a comparison of the experimental with the DFT calculated IR spectrum (Figure 12).

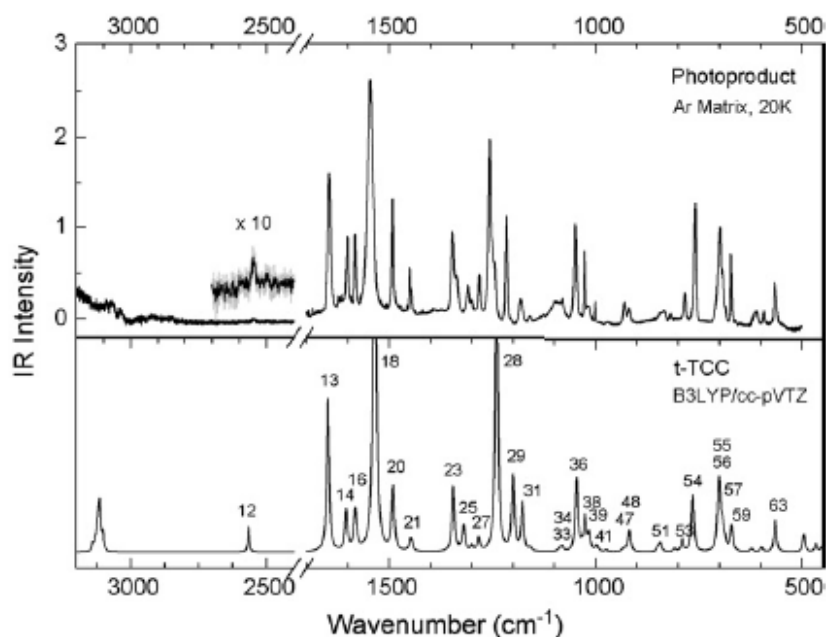


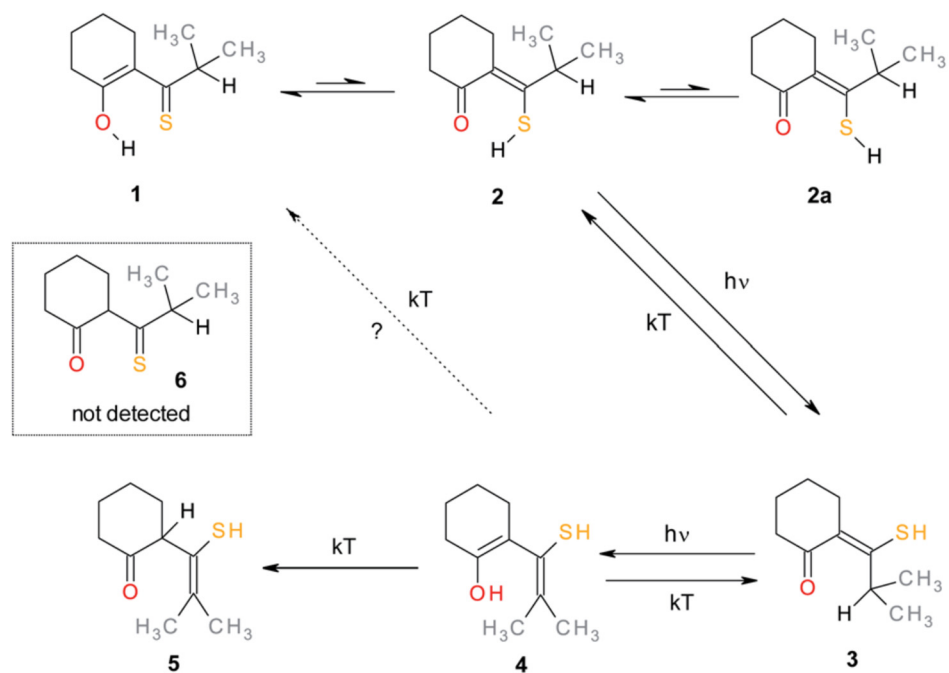
**Figure 12.** Top: Infrared spectrum of open form (t-TCC) obtained after irradiation of **4** in an argon matrix at 20 K. Bottom: Calculated DFT spectrum (B3LYP/cc-pVTZ). Taken from Ref. [85] with permission from Elsevier.

A very efficient way of studying photochromic reactions, in this case for **4**, is to combine laser irradiation with NMR detection (“hyphenation”) typically in one step by using a designed unit of laser, mirrors, and a quartz rod to guide the laser light into the NMR tube [49]. Other setups have been used, as described in Ref [86].

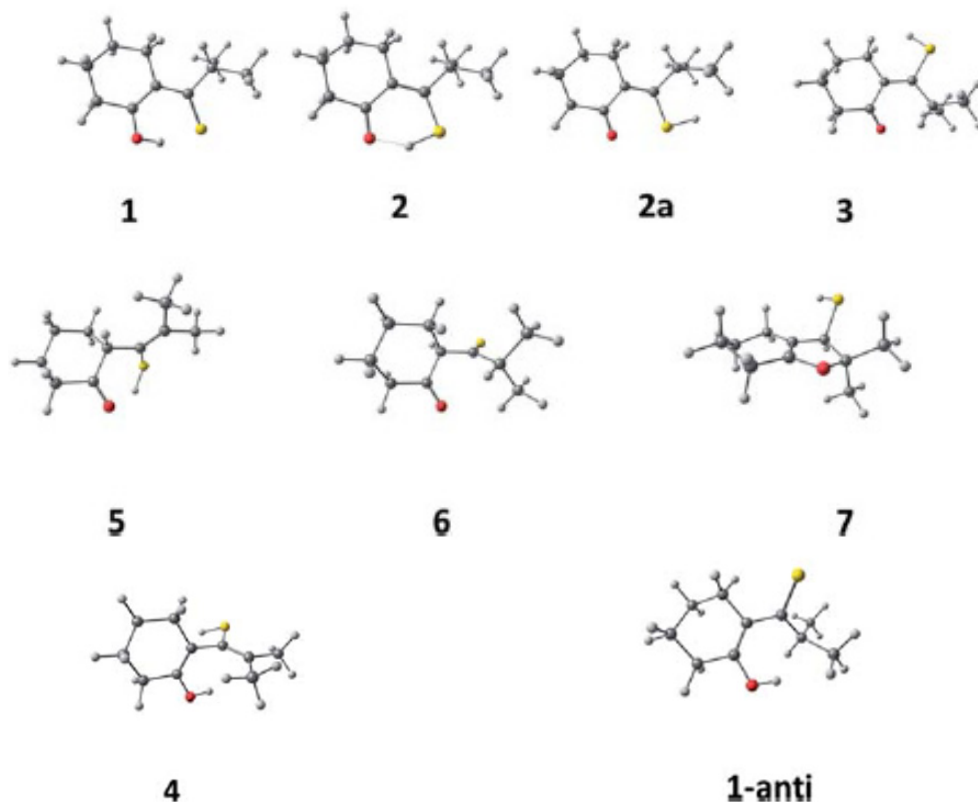
The irradiation of **4** in  $\text{CD}_2\text{Cl}_2$  at 183 K in the NMR instrument leads to a mixture of t-CTC and t-TTC (Scheme 3). It was speculated that the less restrictive matrix allowed the rotated products [49].

The NMR experiments are combined with DFT calculations as well as time-dependent DFT (TD, DFT).

Hyphenated laser-NMR experiments of **5** in  $\text{CD}_2\text{Cl}_2$  at 203 K (irradiation 365 nm) led to the products seen in Scheme 7. Optimized lowest energy structures are seen in Scheme 8. Reaction products with water were also observed.



**Scheme 7.** Irradiation of **5** in a hyphenated experiment. Taken from Ref. [83]. The numbering refers to the RSC article, not to the present paper.



**Scheme 8.** Optimized lowest energy structures of **5**. (Notice the numbering is only local). Taken from Ref. [83].

Doslić and Kühn et al. discussed the laser control of proton transfer in thioacetylacetone and acetylacetone [87].

#### 4. Docking

Docking of small molecules, in this case  $\beta$ -diketones, is a physico-chemical process that may involve hydrogen bonding,  $\pi$ - $\pi$  interactions, steric, hydrophobic, as well as ionic interactions. In case of  $\beta$ -diketones, it is absolutely necessary to know if binding occurs to the keto- or the enol-forms [9]. This seems to not always have been considered. A couple of cases are discussed in Ref. [2]. To get a realistic picture, it is necessary to know the barrier to interconversion and the rate of interconversion between the keto and the enol forms. This has been investigated in a few cases. Conradie et al. [55] determined the rates for thienyl  $\beta$ -diketones. The keto-enol conversion of 3-chloropentane-2,4-dione to the diketo-form was shown to be fast in an aqueous solution of sodium dodecylsulfate (SDS), leading to 65% diketo-form [88]. Curcumin was docked to acetylcholine esterase on the diketo-form, but the enol form was not tested [89].

A very peculiar case is the study of 1-(6-methoxy-2-naphthalene-2-yl)-3-(tosylpyrrolidine-2-yl) propane-1,3-dione (Figure 13), in which the structure all of a sudden is a trans-form (Figure 14) [90].

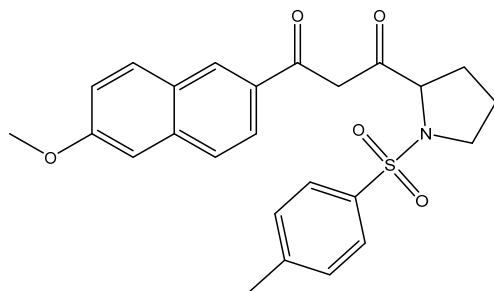


**Figure 13.** Structure of 1-(6-methoxynaphthalene-2-yl)-3-(1-tosylpyrrolidine-2-yl) propane-1,3-dione.

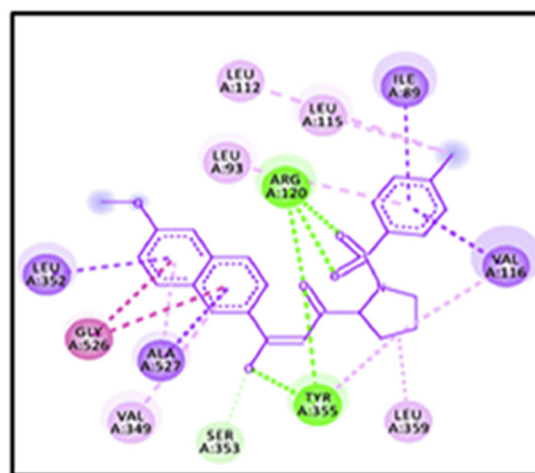


**Figure 14.** Structure of 1-(6-methoxy-2-naphthalene-2-yl)-3-(1-tosylpyrrolidine-2-yl) propane-1,3-dione docked to cyclooxygenase (COX-1). Taken from Ref. [90] with permission from Elsevier.

#### 5. Experimental

NMR. As mentioned earlier we are dealing with a slow equilibrium between diketo and keto-enol forms and a fast equilibrium between the two keto-enols forms (see Scheme 1). The former equilibrium can easily be determined from integrals of  $^1\text{H}$  NMR spectra.] [91]. Tautomeric equilibria may be determined by use of chemical shifts [92]; however, for the latter type, this requires the knowledge of chemical shifts of the individual keto-enol tautomers. A comparison between experimental  $^{13}\text{C}$  chemical shifts and calculated nuclear

shieldings (chemical shifts) is also useful (see Figure 15) [93]. Other similar examples are shown in Ref. [94].

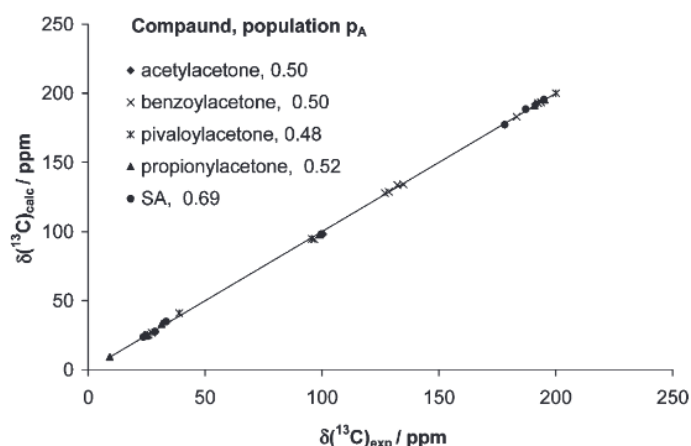


**Figure 15.** Plot of calculated vs. calculated  $^{13}\text{C}$  chemical shifts for  $\beta$ -diketones. Taken from Ref. [93] with permission from the American Chemical Society.

In addition to measurement of chemical shifts, two-bond  $^2J(\text{C},\text{OH})$  coupling constants may also be used to determine tautomeric percentages, as demonstrated for pyridoylbenzoyl  $\beta$ -diketones [64]. Deuteriation, in the present case primarily of the chelate proton, leads, in general, to deuterium isotope effects on chemical shifts and is referred to as intrinsic isotope effects. This type of isotope effect is secondary. Isotope effects on chemical shifts are defined as:

$${}^n\Delta X(\text{h}) = \delta X(\text{l}) - \delta X(\text{h}) \quad (1)$$

where h is the heavy isotope and l the lighter one. N is the number of bonds between the observed nucleus, X, and the isotope.

In asymmetric tautomeric cases, deuteriation leads to a change in the chemical equilibrium, and therefore, to an equilibrium isotope effect on chemical shifts, as described in Equation (3), and a total deuterium isotope effect on chemical shifts, as seen in Equation (4).

$${}^n\Delta X(\text{D})_{\text{int}} = (1 - x_{\text{D}}) {}^n\Delta X(\text{D})_{\text{OH}} + x_{\text{D}} {}^n\Delta X(\text{D})_{\text{NH}} \quad (2)$$

$${}^n\Delta X(\text{D})_{\text{eq}} = (\delta X_{\text{NH}} - \delta X_{\text{OH}}) \Delta x \quad (3)$$

$${}^n\Delta X(\text{D})_{\text{OBS}} = {}^n\Delta X(\text{D})_{\text{int}} + {}^n\Delta X(\text{D})_{\text{eq}} \quad (4)$$

Examples from 1-(2-hydroxyphenyl)-3-aryl-1,3-propanediones (see Scheme 1,  $R_1 = 2\text{-hydroxyphenyl}$  with substituents,  $R_2 = \text{H}$  and  $R_3 = \text{phenyl}$  or substituted naphthalenes) [94]. Deuterium isotope effects on  $^{17}\text{O}$  chemical shifts may also be used. A drawback is the broad lines of  $^{17}\text{O}$  resonances. An advantage is the large chemical shift range.

Isotope effects on chemical shifts are best determined in a one-tube experiment with both the H and the D isotopomer present and with the isotope in slow exchange. However, they may also be determined in protic solvent, but this requires a series of experiments with different degrees of deuterium contents.

Deuteriation at carbon in a symmetric  $\beta$ -diketone may lead to a lifting of degeneracy, as demonstrated in monodeuterated malonaldehyde (Scheme 1,  $R_1$  and  $R_2 = \text{H}$ ,  $R_3 = \text{D}$ ) [95].

For a more detailed review on the use of isotope effects in tautomeric systems, see Ref. [96].

Primary isotope effects have been determined. For  $^2\text{H}$  (D) they are defined as:

$${}^1\Delta \text{H}(\text{D}) = \delta(\text{H}) - \delta(\text{D}) \quad (5)$$

Early on, Altman et al. [97] showed how primary deuterium isotope effects can distinguish between single and double hydrogen bond potential wells. However, if an

equilibrium is at play, this must be considered [96]. Primary deuterium isotope effects may be hampered by the rather broad deuterium resonances. A special case is the determination of tritium primary isotope effects. Tritiation gives both sharp resonances and larger isotope effects, but the drawback is the difficulty of finding a tritium enrichment facility and the fact that the samples deteriorate over time.

A comparison of the different types of isotope effects are shown in Figure 16.

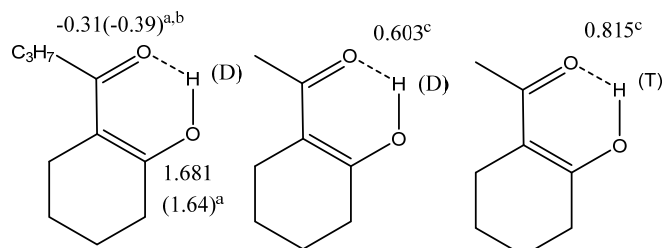


**Figure 16.** Deuterium isotope effects on chemical shifts in ppm. a. The values in brackets are for 2-acetylcyclohexanone. b. From Ref. [98]. c. From Ref. [99].

For tautomeric systems, the isotope effects on chemical shifts may vary strongly with temperature. This is seen from Figure 17, and is related to the dependence of the mole fraction, as seen in Figure 18 [99].

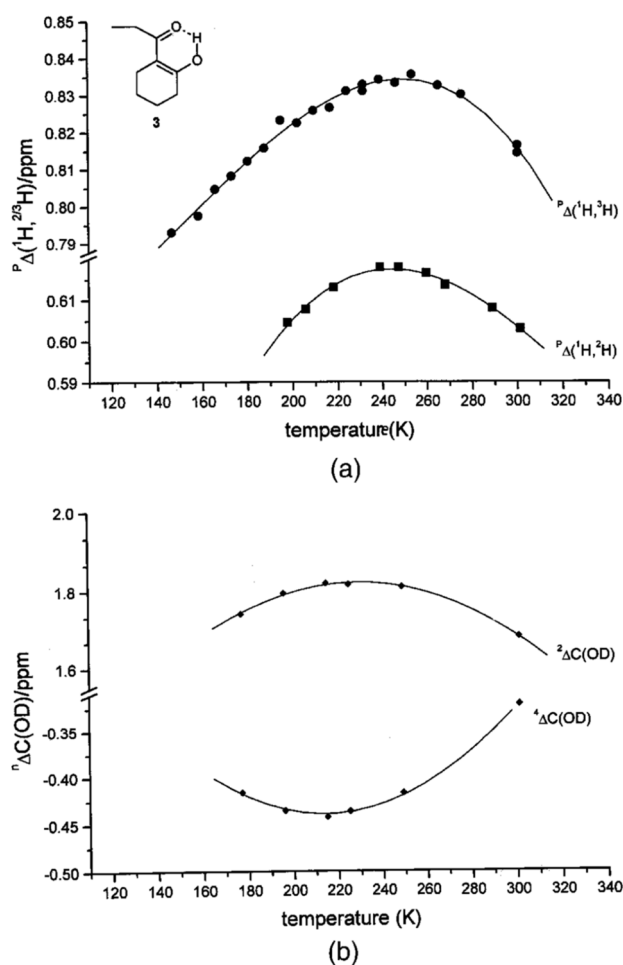


**Figure 17.** Top: Primary tritium, deuterium isotope effects. Bottom: Deuterium isotope effects on  $^{13}\text{C}$  chemical shifts. Taken from Ref. [98] with permission from John Wiley and sons.

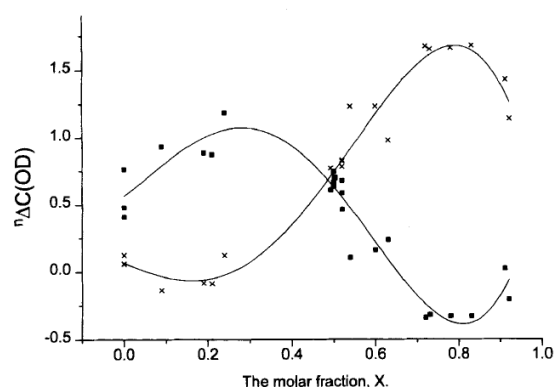


**Figure 18.** Dependence of deuterium isotope effects on chemical shifts in  $\beta$ -diketones as a function of the mole fraction. Taken from Ref. [99] with permission from John Wiley and sons.

## 6. Conclusions

An important physico-chemical feature of  $\beta$ -diketones and  $\beta$ -thioxoketones is clearly tautomerism. In the case of  $\beta$ -diketones, both an enol and a diketo-form exist. Studies are conducted both in the liquid and in the solid state. In the liquid state, the present techniques can usually establish the dominant form of  $\beta$ -diketones, whereas in the solid state, tautomerism is much more difficult to establish. There is a need to have a much clearer picture of the dependence of the hydrogen bond potential form of the  $\beta$ -diketones as a function of structure and temperature.

For  $\beta$ -thioxoketones, deuterium isotope effects on chemical shifts have proven useful due to the large chemical shift differences between identical nuclei in the two tautomers.

In case of docking studies, it is important to establish the correct tautomer [9] and is even more important to determine the barrier to interconversion between tautomers.

The study of the excited state has taken a great leap forward; however, especially for  $\beta$ -thioxoketones, there is a need for a full picture and, likewise, to investigate the use of photochemically excited molecules in reactions, e.g., with oxygen, but these kind of studies could also be extended to other reagents. The use of  $\beta$ -diketones elements in molecules for OLED's has proven useful; however, to reach the full potential, more research is needed.

**Funding:** This research received no external funding.

**Institutional Review Board Statement:** Not applicable.

**Informed Consent Statement:** Not applicable.

**Data Availability Statement:** Not applicable.

**Conflicts of Interest:** The author declares no conflict of interest.

## References

- De Gonzalo, G.; Alcántara, A.R. Recent Development in the Synthesis of  $\beta$ -diketones. *Pharmaceuticals* **2021**, *14*, 1043.
- Hansen, P.E. Structural Studies of  $\beta$ -diketones and its implications on Biological Effects. *Pharmaceuticals* **2021**, *14*, 1189. [CrossRef]
- Kljun, J.; Ture, I.  $\beta$ -Diketones as Scaffolds for Anticancer Drug Design—From Organic Building Blocks to Natural Products and Metallodrug Components. *Eur. J. Inorg. Chem.* **2017**, *12*, 1655–1666. [CrossRef]
- Anand, P.; Thomas, S.G.; Kunnumakkara, A.B.; Sundaram, C.; Harikumar, K.B.; Sung, B.; Tharakan, S.T.; Misra, K.; Priyadarsini, I.K.; Rajasekharan, K.N. Biological activities of curcumin and its analogues (Congeners) made by man and Mother. *Nat. Biochem. Pharmacol.* **2008**, *76*, 1590–1611. [CrossRef]
- Nelson, K.M.; Dahlin, J.L.; Bisson, J.; Graham, J.; Pauli, G.F.; Walters, M.A. The Essential Medicinal Chemistry of Curcumin. *J. Med. Chem.* **2017**, *60*, 1620–1637. [CrossRef]
- Priyadarsini, K.I. Chemical and Structural Features Influencing the Biological Activity of Curcumin. *Curr. Pharm. Des.* **2013**, *19*, 2093–2100.
- Slika, L.; Patra, D. A short review on chemical properties, stability and nano-technological advances for curcumin delivery. *Expert Opin. Drug Deliv.* **2020**, *17*, 61–75. [CrossRef]
- Malekshah, R.E.; Salehi, M.; Kubicki, M.; Khaleghian, A.J. Biological studies and computational modeling of two new copper complexes derived from  $\beta$ -diketones and their nano-complexes. *Coord. Chem.* **2019**, *72*, 1697–1714. [CrossRef]

9. Hansen, P.E.; Mortensen, J.; Kamounah, F.S. The importance of correct tautomeric structures for biological molecules. *JSM Chem.* **2015**, *3*, 1014–1019.
10. Jezierska, A.; Panek, J.J. Investigation of an O-H . . . S hydrogen bond via Carr-Parrinello and Path Integral molecular dynamics. *J. Comput. Chem.* **2009**, *30*, 1241–1250. [[CrossRef](#)]
11. Mayoral, M.J.; Cornago, P.; Claramunt, R.; Cano, M. Pyridyl and pyridiniumyl  $\beta$ -diketonates as building blocks for palladium(III) and allyl-platinum(II) isomers. Multinuclear NMR structural elucidation and liquid crystal behavior. *New. J. Chem.* **2011**, *35*, 1020–1030. [[CrossRef](#)]
12. Andrews, P.C.; Blair, V.L.; Ferrero, R.L.; Junk, P.C.; Kedzierski, L.; Peiris, R.M. Bismuth(III) beta-thioxoketonates as antibiotics against *Helicobacter pylori* and as anti-leishmanial agents. *Dalton Trans.* **2014**, *43*, 1279–1291. [[CrossRef](#)]
13. Duus, F.; Antonsen, J.W. Thioxoketones. I. Preparation and Structure of Thioacetylacetone. *Acta Chem. Scand.* **1977**, *B 31*, 40–46. [[CrossRef](#)]
14. Semenova, I.S.; Yarovenko, V.N.; Levchenko, K.S.; Krayushkin, M.M. Synthesis of 1,3-thioxoketones from salicylaldehyde. *Russ. Chem. Bull.* **2013**, *62*, 1022–1025. [[CrossRef](#)]
15. Becke, A.D. Density functional thermochemistry. III. The role of exact exchange. *J. Chem. Phys.* **1993**, *98*, 5648–5652. [[CrossRef](#)]
16. Lee, C.; Yang, W.; Parr, R.G. Development of the Colle-Salvetti correlation-energy formula into a functional of the electron density. *Phys. Rev. B* **1988**, *37*, 785–789. [[CrossRef](#)]
17. Belova, N.V.; Oberhammer, H.; Trang, N.H.; Girichev, G.V. Tautomeric Properties and Gas-Phase Structure of Acetylacetone. *J. Org. Chem.* **2014**, *79*, 5412–5419. [[CrossRef](#)]
18. Belova, N.V.; Oberhammer, H.; Girichev, G.V. Tautomeric and conformational properties of dibenzoylmethane, C<sub>6</sub>H<sub>5</sub>-C(O)-CH<sub>2</sub>-C(O)-C<sub>6</sub>H<sub>5</sub>: Gas-phase electron diffraction and quantum chemical study. *Struct. Chem.* **2011**, *22*, 269–277. [[CrossRef](#)]
19. Belova, N.V.; Oberhammer, H.; Girichev, G.V.; Shlykov, S.A. Automeric properties and gas-phase structure of 3-chloro-2,4-pentanedione. *J. Phys. Chem. A* **2008**, *112*, 3209–3214. [[CrossRef](#)]
20. Belova, N.V.; Trang, N.H.; Trang, N.H.; Girichev, G.V. Tautomeric and conformational properties of dipivaloylmethane. *J. Mol. Struct.* **2017**, *1132*, 63–69. [[CrossRef](#)]
21. Gilli, G.; Gilli, P. Towards an unified hydrogen-bond theory. *J. Mol. Struct.* **2000**, *552*, 1–15. [[CrossRef](#)]
22. Anjomshoa, S.; Namazian, M.; Noorbala, M.R. The Effect of Solvent on Tautomerism, Acidity and Radical Stability of Curcumin and Its Derivatives Based on Thermodynamic Quantities. *J. Sol. Chem.* **2016**, *45*, 1021–1030. [[CrossRef](#)]
23. Sandler, I.; Harper, J.B.; Ho, J. Explanation of Substituent Effects on the Enolization of  $\beta$ -Diketones and  $\beta$ -Ketoesters. *J. Chem. Educ.* **2021**, *98*, 1043–1048. [[CrossRef](#)]
24. Cortney, C.H.; Krishnan, V.V. Keto–Enol Tautomerization of Acetylacetone in Mixed Solvents by NMR Spectroscopy. A Physical Chemistry Experiment on the Application of the Onsager-Kirkwood Model for Solvation Thermodynamics. *J. Chem. Educ.* **2020**, *97*, 825–830. [[CrossRef](#)]
25. Schweitzer, G.K.; Benson, W. Enol Content of Some Beta-Diketones. *J. Chem. Eng. Data* **1968**, *3*, 454–455.
26. Sloop, J.C.; Boyle, P.D.; Fountain, A.W.; Pearman, W.F.; Swann, J.A. Electron-Deficient Aryl beta-Diketones: Synthesis and Novel Tautomeric Preferences. *Eur. J. Org. Chem.* **2011**, 936–941. [[CrossRef](#)]
27. Belova, N.V.; Sliznev, V.V.; Oberhammer, H.; Girichev, G.V. Tautomeric and conformational properties of beta-diketones. *J. Mol. Struct.* **2010**, *978*, 282–293. [[CrossRef](#)]
28. Zawadiak, J.; Mrzyczek, M. UV absorption and keto-enol tautomerism equilibrium of methoxy and dimethoxy 1,3-diphenylpropane-1,3-diones. *Spectrochim. Acta. A Mol. Biomol. Spectrosc.* **2010**, *75*, 925–929. [[CrossRef](#)]
29. Manolova, Y.; Deneva, V.; Antonov, L.; Drakalska, E.; Momekova, D.; Lambov, N. The effect of the water on the curcumin tautomerism: A quantitative approach. *Spectrochim. Acta A Mol. Biomol. Spectrosc.* **2014**, *132*, 815–820. [[CrossRef](#)]
30. Adeniyi, A.A.; Conradie, J. The stability, kinetics and inter-fragment electron communication of the tautomers of twelve selected beta-diketone molecules: A computational study. *J. Mol. Graph. Model.* **2018**, *85*, 25–39. [[CrossRef](#)]
31. Henry, M.C.; Yonker, C.R. FT-IR studies of acetylacetonates in supercritical CO<sub>2</sub> using a capillary cell at pressures up to 3.1 kbar. *Anal. Chem.* **2004**, *76*, 4684–4689. [[CrossRef](#)]
32. Levina, E.O.; Khrenova, M.G.; Astakhov, A.A.; Tsirelson, V.G. Keto-enol tautomerism from the electron delocalization perspective. *J. Comput. Chem.* **2022**, *43*, 1000–1010. [[CrossRef](#)] [[PubMed](#)]
33. Roy, R.; Biswas, S.; Pramanik, A.; Sarkar, P. Computational Studies on the Keto-Enol Tautomerism of Acetylacetone. *Int. J. Res. Soc. Nat. Sci.* **2017**, *2*, 2455–5916.
34. Tsukahara, T.; Nagaoka, K.; Morikawa, K.; Mawatari, K.; Kitamori, T. Keto–Enol Tautomeric Equilibrium of Acetylacetone Solution Confined in Extended Nanospaces. *J. Phys. Chem. B* **2015**, *119*, 14750–14755. [[CrossRef](#)] [[PubMed](#)]
35. Tayyari, S.F.; Najafi, A.; Lorestani, F.; Sammelson, R.E. Hydrogen bond strength and vibrational assignment of the enol form of 3-(methylthio)pentane-2,4-dione. *J. Mol. Struct.-Theochem.* **2008**, *854*, 54–62. [[CrossRef](#)]
36. Sammelson, R.E.; Najafi, A.; Lorestani, F.; Azizkhani, M.; Tayyari, S.F. Hydrogen bond strength and vibrational assignment of the enol form of 3-(phenylthio)pentane-2,4-dione. *J. Mol. Struct.* **2008**, *889*, 165–176. [[CrossRef](#)]
37. Dolati, F.; Tayyari, S.F.; Vakili, M. Tautomerism, conformational analysis, and spectroscopy studies of 3-bromo-pentane-2,4-dione. *J. Mol. Struct.* **2015**, *1094*, 264–273. [[CrossRef](#)]
38. Zahedi-Tabrizi, M.; Tayyari, F.; Moosavi-Tekyeh, Z.; Jalali, A.; Tayyari, S.F. Structure and vibrational assignment of the enol form of 1,1,1-trifluoro-2,4-pentanedione. *Spectrochim. Acta A-Mol. Biomol. Spectros.* **2006**, *65*, 387–396. [[CrossRef](#)]

39. Cornago, P.; Claramunt, R.M.; Bouissane, L.; Alkorta, I.; Elguero, J. A study of the tautomerism of beta-dicarbonyl compounds with special emphasis on curcuminoids. *Tetrahedron* **2008**, *64*, 8089–8094. [[CrossRef](#)]
40. Carlsen, L.; Hansen, P.E.; Saeed, B.A.; Elias, R.S. Curcumin analogues for possible cancer treatment. A QSAR study. *World J. Biol. Pharm. Res.* **2021**, *1*, 1–16. [[CrossRef](#)]
41. Mennucci, B.; Tomasi, J.; Cammi, R.; Cheeseman, J.R.; Frisch, M.J.; Devlin, F.J.; Gabriel, S.; Stephens, P.J. Polarizable Continuum Model (PCM) Calculations of Solvent Effects on Optical Rotations of Chiral Molecules. *J. Phys. Chem. A* **2002**, *106*, 6102–6113. [[CrossRef](#)]
42. Takano, Y.; Houk, K.N. Benchmarking the Conductor-like Polarizable Continuum Model (CPCM) for Aqueous Solvation Free Energies of Neutral and Ionic Organic Molecules. *J. Chem. Theory Comput.* **2005**, *1*, 70–77. [[CrossRef](#)] [[PubMed](#)]
43. Marenich, A.V.; Cramer, C.J.; Truhlar, D.G. Universal solvation model based on solute electron density and on a continuum model of the solvent defined by the bulk dielectric constant and atomic surface tensions. *J. Phys. Chem. B* **2009**, *113*, 6378–6396. [[CrossRef](#)] [[PubMed](#)]
44. Mehrani, S.; Tayyari, S.F.; Herav, M.M.; Morsali, A. Theoretical investigation of solvent effect on the keto-enol tautomerization of pentane-2,4-dione and a comparison between experimental data and theoretical calculations. *Can. J. Chem.* **2021**, *99*, 411–424. [[CrossRef](#)]
45. Bader, R.F.W. *Atoms in Molecules: A Quantum Theory*; Oxford University Press: Oxford, UK, 1990.
46. Casier, B.; Sisourat, N.; Carniato, S.; Capron, N. Keto-enol tautomerism in micro-hydrated acetylacetone: An atoms-in-molecules study. *Theor. Chem. Acc.* **2018**, *137*, 1–10. [[CrossRef](#)]
47. Serdiuk, I.E.; Wera, M.; Roshal, A.S.D.; Sowinsky, P.; Zadykowicz, B. Tautomerism, structure and properties of 1,1',1''-(2,4,6-trihydroxybenzene-1,3,5-triyl)triethanone. *Tetrahedron Lett.* **2011**, *52*, 2737–2740. [[CrossRef](#)]
48. Hansen, P.E.; Kamounah, F.S.; Zhiryakova, D.; Manolova, Y.; Antonov, L. 1,1',1''-(2,4,6-hydroxybenzene-1,3,5-triyl)triethanone non-tautomerism. *Tetrahedron Lett.* **2014**, *55*, 354–357. [[CrossRef](#)]
49. Waluk, J.; Pietrzak, M.; Dobkowski, J.; Gorski, A.; Gawinkowski, S.; Kijak, M.; Luboradzki, R.; Hansen, P.E. Arresting consecutive steps of a photochromic reaction: Studies of  $\beta$ -thioxoketones combining laser photolysis with NMR detection. *Chem. Phys. Phys. Chem.* **2014**, *16*, 9128–9137.
50. Kong, X.; Brinkmann, A.; Terskikh, V.; Wasylishen, R.E.; Bernard, G.M.; Duan, Z.; Wu, Q.; Wu, G. Proton Probability Distribution in the O...H...H Low-Barrier Hydrogen Bond: A Combined Solid-State NMR and Quantum Chemical Computational study of Dibenzoylmethane and Curcumin. *J. Phys. Chem. B* **2016**, *120*, 11692–11704. [[CrossRef](#)]
51. Herstein, F.H.; Iversen, B.B.; Kapon, M.; Krebs Larsen, F.; Madsen, G.K.H.; Reiser, G.M. X-ray and neutron diffraction study of benzoylacetone in the temperature range 8–300 K: Comparison with other *cis*-enol molecules. *Acta Cryst.* **1999**, *B55*, 767–787. [[CrossRef](#)]
52. Thomas, L.H.; Florence, A.J.; Wilson, C.C. Hydrogen atom behavior imaged in a short intramolecular hydrogen bond using the combined approach of X-ray and neutron diffraction. *New J. Chem.* **2009**, *33*, 2486–2490. [[CrossRef](#)]
53. Srinivasan, R.; Feenstra, J.S.; Park, S.T.; Xu, S.; Zewail, A.H. Direct determination of hydrogen-bonded structures in resonant and tautomeric reactions using ultrafast electron diffraction. *J. Am. Chem. Soc.* **2004**, *126*, 2266–2267. [[CrossRef](#)]
54. Clark, S.J.; Segall, M.D.; Pickard, C.J.; Hasnip, P.J.; Probert, M.I.J.; Refson, K.; Payne, M.C. First principles methods using CASTEP. *Z. Kristallogr.* **2005**, *220*, 567–570. [[CrossRef](#)]
55. Conradie, M.M.; Muller, A.J.; Conradie, J. Thienyl-containing  $\beta$ -Diketones: Synthesis, Characterization, Crystal structure and Keto-enol Kinetics. *S. Afr. J. Chem.* **2008**, *61*, 13–21.
56. Nieto, C.I.; Cabildo, P.; Claramunt, R.M.; Carnago, P.; Sanz, D.; Torralba, M.C.; Torres, M.R.; Ferraro, M.B.; Alkorta, I.; Marín-Luna, M.; et al. The structure of  $\beta$ -diketones related to curcumin determined by X-ray crystallography, NMR (solution and solid state) and theoretical calculations. *Strukt. Chem.* **2016**, *27*, 705–730. [[CrossRef](#)]
57. Jiménez-Cruz, F.; Mar, L.F.; García-Gutierrez, J.L. Molecular structure and OAHO hydrogen bond in 1-aryl-1,3-diketone malonates. *J. Mol. Struct.* **2013**, *1034*, 43–50. [[CrossRef](#)]
58. Babjakova, E.; Dastychova, L.; Hanulíková, B.; Kuřitka, I.; Nečas, M.; Vašková, H.; Vicha, R. Synthesis, molecular structure and vibrational spectra of 1,3-bis(1-adamantyl)-2-phenylpropan-1,3-diones. *J. Mol. Struct.* **2015**, *1085*, 207–214. [[CrossRef](#)]
59. Chatterjee, C.; Incarvito, C.D.; Burns, L.A.; Vaccaro, P.H. Electronic Structure and Proton Transfer in Ground-State Hexafluoroacetylacetone. *J. Phys. Chem. A* **2010**, *114*, 6630–6640. [[CrossRef](#)]
60. Oyarce, J.; Hernandez, L.; Ahumada, G.; Soto, J.P.; Del Valle, M.A.; Dorcet, V.; Carrillo, D.; Hamon, J.-R.; Manzur, C. Thiophene-containing beta-diketonate complex of copper(II): X-ray crystal structure and electropolymerization. *Polyhedron* **2017**, *123*, 277–284. [[CrossRef](#)]
61. Car, R.; Parrinello, M. Unified Approach for Molecular Dynamics and Density-Functional Theory. *Phys. Rev. Lett.* **1985**, *55*, 2471–2474. [[CrossRef](#)]
62. Marx, D.; Parrinello, M. Ab initio path integral molecular dynamics: Basic ideas. *J. Chem. Phys.* **1996**, *104*, 4077–4082. [[CrossRef](#)]
63. Durlak, P.; Latajka, Z. Car-Parrinello and path integral molecular dynamics study of the intramolecular hydrogen bonds in the crystals of benzoylacetone and dideuterobenzoylacetone. *Phys. Chem. Chem. Phys.* **2014**, *16*, 23026–23037. [[CrossRef](#)]
64. Hansen, P.E.; Borisov, E.V.; Lindon, J.C. Determination of the Tautomeric Equilibria of Pyridoyl Benzoyl  $\beta$ -Diketones in the Liquid and Solid State through the use of Deuterium Isotope Effects on  $^1\text{H}$  and  $^{13}\text{C}$  NMR Chemical Shifts and Spin Coupling Constants. *Spectrochim. Acta* **2015**, *136*, 107–112. [[CrossRef](#)]

65. Dudek, M.; Clegg, J.K.; Glasson, C.R.K.; Kelly, N.; Gloe, K.; Gloe, K.; Kelling, A.; Buschmann, H.-J.; Jolliffe, K.A.; Lindoy, L.F.; et al. Interaction of Copper(II) with Ditopic Pyridyl- $\beta$ -diketone Ligands: Dimeric, Framework, and Metallogel Structures. *Cryst. Growth DES* **2011**, *11*, 1697–1704. [[CrossRef](#)]
66. Martinez, V.; Bedeković, N.; Stilinović, V.; Cincic, D. Tautomeric Equilibrium of an Asymmetric  $\beta$ -diketone in Halogen-Bonded Cocrystals with perfluorinated iodo benzenes. *Crystal* **2021**, *11*, 699. [[CrossRef](#)]
67. Wasylshen, R.E.; Matlinska, M.A.; Bernard, G.M.; Terskikh, V.V.; Brinkmann, A. Hydrogen-Bonding in the Enol Tautomer of 1,3-Diketones: Insights from 2/1H Isotope Effects on NMR Parameters in the Solid State as well as Computational Chemistry. *Acta Cryst.* **2019**, *A75*, a292. [[CrossRef](#)]
68. Bolvig, S.; Hansen, P.E.; Wemmer, D.; Williams, P. Deuterium Isotope Effects on  $^{17}\text{O}$  Chemical Shifts of Intramolecularly Hydrogen Bonded Systems. *J. Mol. Struct.* **1999**, *509*, 171–181. [[CrossRef](#)]
69. Noerskov-Lauritsen, L.; Carlsen, L.; Duus, F. Definitive Evidence for the Existence of the Hydrogen-bonding Enol Form of Non-aromatic  $\beta$ -Thioxoketones. X-Ray Crystal Structure of I-(I-Methylcyclopropyl)-3-thioxobutan-1-one. *J. Chem. Soc. Chem. Commun.* **1983**, *9*, 496–498. [[CrossRef](#)]
70. Rozatian, N.; Beeby, A.; Ashworth, I.W.; Sandford, G.; Hodgson, D.R.W. Enolization rates control mono-versus di-fluorination of 1,3-dicarbonyl derivatives. *Chem. Sci.* **2019**, *10*, 10318–10330. [[CrossRef](#)]
71. Kojic, M.; Petkovic, M.; Etinski, M. A new insight into the photochemistry of avobenzene in gas phase and acetonitrile from ab initio calculations. *Phys. Chem. Chem. Phys.* **2016**, *18*, 22168–22178. [[CrossRef](#)]
72. Suwa, Y.; Yamaji, M. Steady state and laser photolysis studies of keto-enol tautomerizations in 2-alkyl-1,3-diketones having five-membered rings in acetonitrile: Temporal UV-A sunscreen. *J. Photochem. Photobiol. A Chem.* **2016**, *316*, 69–74. [[CrossRef](#)]
73. Chi, T.X.-C.; Wang, Y.-H.; Gao, Y.; Sui, N.; Zhang, L.-Q.; Wang, W.-Y.; Lu, R.; Ji, W.-Y.; Yang, Y.-Q.; Zhang, H.-Z. Acceptor number-dependent ultrafast photo-physical properties of push-pull chromophores using time-resolved methods. *Chem. Phys. Lett.* **2018**, *698*, 127–131. [[CrossRef](#)]
74. Verma, P.K.; Steinbacher, A.; Koch, F.; Nuernberger, P.; Brixner, T. Monitoring Ultrafast Intramolecular proton Transfer Processes in an Unsymmetrical  $\beta$ -Diketone. *Phys. Chem. Chem. Phys.* **2015**, *17*, 8459–8466. [[CrossRef](#)] [[PubMed](#)]
75. Verma, P.K.; Steinbacher, A.; Koch, F.; Nuernberger, P.; Brixner, T. Excited-state Intramolecular proton transfer of 2-acetylandan-1,3-dione studied by ultrafast absorption and fluorescence spectroscopy. *Struct. Dyn.* **2016**, *3*, 023606. [[CrossRef](#)] [[PubMed](#)]
76. Li, M.; Ren, W.; He, Z.; Zhu, Y. The Investigation of Excited-State Intramolecular proton transfer Mechanism of 2-acetyl-1,3-Dion: The solvation effect. *J. Clust. Sci.* **2017**, *28*, 2111–2122. [[CrossRef](#)]
77. Wu, K.; Zhang, T.; Wang, Z.; Wang, L.; Zhan, L.; Gong, S.; Zhong, C.; Lu, Z.-H.; Zhang, S.; Yang, C. Do Novo Design of Excited-State Intramolecular Proton Transfer Emitters via a Thermally Activated Delayed fluorescence Channel. *J. Am. Chem. Soc.* **2018**, *140*, 887–8886.
78. Leen, V.; Laine, M.; Ngongo, J.M.; Lipkowski, P.; Verbelen, B.; Kochel, A.; Dehaen, W.; Van der Auweraer, M.; Nadochenko, V.; Filarowski, A. Impact of the Keto–Enol Tautomeric Equilibrium on the BODIPY Chromophore. *J. Phys. Chem. A* **2018**, *122*, 5955–5961. [[CrossRef](#)]
79. Tang, B.; Zhang, H.; Cheng, X.; Ye, K.; Zhang, H. 1,3-Diaryl- $\beta$ -diketone Organic Crystals with Red Amplified Spontaneous Emission. *ChemPlusChem* **2016**, *81*, 1320–1325. [[CrossRef](#)]
80. Cheg, X.; Li, F.; Han, S.; Zhang, Y.; Jiao, C.; Wei, J.; Ye, K.; Wang, Y.; Zhang, H. Emission behaviors of unsymmetrical 1,3-diaryl- $\beta$ -diketones: A model perfectly disclosing the effect of molecular conformation on luminescence of organic solids. *Sci. Rep.* **2015**, *5*, 9140.
81. Wu, D.; Fang, X.; Song, J.; Qu, L.; Zhou, X.; Xiang, H.; Wang, J.; Liu, J.J. Multi-stimuli-responsive fluorescence of axially chiral 4-en- $\beta$ -diketones. *Dye. Pigment.* **2021**, *184*, 108851. [[CrossRef](#)]
82. Andresen, B.; Duus, F.; Bolvig, S.; Hansen, P.E. Variable Temperature  $^1\text{H}$  and  $^{13}\text{C}$  NMR Spectroscopic Investigation of the Enol-Enethiol tautomerism of  $\beta$ -Thioxoketones. Isotope Effects due to Deuteron Chelation. *J. Mol. Struct.* **2000**, *552*, 45–63. [[CrossRef](#)]
83. Pietrzak, M.; Buczyńska, J.; Duus, F.; Waluk, J.; Hansen, P. Photoinduced and Ground State Conversions in a Cyclic  $\beta$ -Thioxoketone. *RSC Adv.* **2022**, *12*, 681–689. [[CrossRef](#)]
84. Posokhov, A.; Gorsky, A.; Spanget-Larsen, J.; Duus, F.; Hansen, P.E.; Waluk, J. The Structure of the Phototransformation product in monothiodibenzoylmethane. *Chem. Phys. Lett.* **2001**, *350*, 502–508. [[CrossRef](#)]
85. Hansen, B.K.V.; Gorski, A.; Posokhov, Y.; Duus, F.; Hansen, P.E.; Waluk, J.; Spanget-Larsen, J. Monothiodibenzoylmethane: Structural and vibrational assignments. *Vib. Spectros.* **2007**, *43*, 53–63. [[CrossRef](#)]
86. Nitschke, P.; Lokesh, N. Combination of illumination and high resolution NMR spectroscopy: Key features and practical aspects, photochemical applications, and new concepts. *Progr. NMR* **2019**, *114–115*, 86–134. [[CrossRef](#)]
87. Doslić, N.; Abdel-Latif, M.K.; Kühn, O. Laser control of single and double proton transfer reactions. *Acta Chim. Slov.* **2011**, *58*, 411–424.
88. Iglesias, E. Substituent effects on enol nitrosation of 1,3-diketones. *Int. J. Chem. Kin.* **2012**, *44*, 668–679. [[CrossRef](#)]
89. Parameswari, A.R.; Rajalakshmi, G.; Kumaradhas, P. A combined molecular docking and charge density analysis is a new approach for medicinal research to understand drug-receptor interaction: Curcumin-AChE model. *Chem. Biol. Interact.* **2015**, *225*, 21–31. [[CrossRef](#)]
90. Porchezhiyan, V.; Kalaivani, D.; Sobana, J.; Noorjahan, S.E. Synthesis, docking and in vitro evaluation of L-proline derived 1,3-diketones possessing anti-cancer and anti-inflammatory activities. *J. Mol. Struct.* **2020**, *1206*, 127754. [[CrossRef](#)]
91. Manbeck, K.A.; Boaz, N.C.; Bair, N.C.; Sanders, A.M.S.; Marsh, A.L. Substituent Effects on Keto-Enol Equilibria Using NMR Spectroscopy. *J. Chem. Educ.* **2011**, *88*, 1444–1445. [[CrossRef](#)]

92. Claramunt, R.M.; López, C.; Maria, M.D.S.; Sanz, D.; Elguero, J. The use of NMR spectroscopy to study tautomerism. *Prog. Nucl. Magn. Reson. Spectrosc.* **2006**, *49*, 169–206. [[CrossRef](#)]
93. Bal, D.; Kraska-Dziadecka, A.; Gryff-Keller, A. Solution Structure of Succinylacetone, An Unsymmetrical beta-Diketone, As Studied by C-13 NMR and GIAO-DFT Calculations. *J. Org. Chem.* **2009**, *74*, 8604–8609. [[CrossRef](#)] [[PubMed](#)]
94. Buceta, N.N.; Della Ve´dova, C.O.; Romanelli, G.P.; Autino, J.C.; Jios, J.L. Deuterium isotopic effect on <sup>13</sup>C NMR chemical shifts of 1-(2-hydroxyphenyl)-3-aryl-1,3-propanediones: Hydrogen bond and substituent effects. *J. Mol. Struct.* **2008**, *878*, 50–59. [[CrossRef](#)]
95. Perrin, C.L.; Kim, Y.J. Symmetry of the hydrogen bond in malonaldehyde enol in solution. *J. Am. Chem. Soc.* **1998**, *120*, 12641–12645. [[CrossRef](#)]
96. Hansen, P.E. Methods to distinguish tautomeric cases from static ones. In *Tautomerism: Ideas, Compounds, Applications*; Antonov, L., Ed.; Wiley-VCH: Weinheim, Germany, 2016.
97. Altman, L.J.; Laungani, D.; Gunnarsson, G.; Wennerström, H.; Forsén, S. Proton, deuterium and tritium nuclear magnetic-resonance of intra-molecular hydrogen bonds—isotope effects and shape of potential-energy function. *J. Am. Chem. Soc.* **1978**, *100*, 8264–8266. [[CrossRef](#)]
98. Bolvig, S.; Hansen, P.E.; Morimoto, H.; Wemmer, D.; Williams, P. Primary Tritium and Deuterium Isotope Effects on Chemical Shifts of Compounds having an Intramolecular Hydrogen bond. *Magn. Reson. Chem.* **2000**, *38*, 525–535. [[CrossRef](#)]
99. Bolvig, S.; Hansen, P.E. Deuterium Isotope Effects on <sup>13</sup>C Chemical Shifts as a Probe for Tautomerism in Enolic β-Diketones. *Magn. Reson. Chem.* **1996**, *34*, 467–478. [[CrossRef](#)]

**Disclaimer/Publisher’s Note:** The statements, opinions and data contained in all publications are solely those of the individual author(s) and contributor(s) and not of MDPI and/or the editor(s). MDPI and/or the editor(s) disclaim responsibility for any injury to people or property resulting from any ideas, methods, instructions or products referred to in the content.